Simulation of Effective Thermal Diffusivity in a Two-hase Material

BY ANDREW PULLIN

The effective thermal diffisuvity of a two-phase material comprised of a matrix and sphereical particles is investigated by direct simulation. A representative volume element is subjeted to a isothermal gradient boundary condition across the thickness. A hardware accelerated finite differences solver is used to solve the thermal diffusivity equation over the RVE for the steady state temperature distribution. Post-processing gives the effective composite thermal diffusivity. A parameter study is conducted across a range of values of relative particle size and relative mismatch of the thermal difficuity of each individual phase.

Keywords: Thermal diffusivity, GPU, Parametric study

1. Introduction

This project seeks to investigate the effective thermal diffusivity of a material that is intended to model a sintered thermoelectric engineered material. The implementation in this project is not specific to this application, and provides a generalize invetigation of the thermal performance of a representative volume element (RVE) with a particle phase included.

The material in this analysis will be modeled as a binder matrix material, called "Phase 1", with thermal diffusivity κ_1, with sphereical included particles, called "Phase 2",with thermal diffusivity κ_2. The materials of each phase are assumed to be isotropic. Dense packing of the particle spheres was not implemented; a "random insertion" algorithm was used, with a stopping condition on the number of unsuccesful attempts to insert each next particle into the set.

2. Objectives

The objective of this project is to determine the effective thermal diffusivity, κ^*, of a RVE of the considered two-phase material as a function of two dimensionalized parameters that represent the properties of the included particle phase.

A paremetric study of two parameters will be conducted. With appropriate choice of nondimensional parameters, this problem can be largely generalize. The selected parameters are the ratio of the particle radius to the edge length of a cubic domain and the mismatch ratio between κ_1 and κ_2. Specifically:

$$\begin{aligned} \eta &= \frac{R}{V^(1/3)} \\ \alpha &= \frac{\kappa_2}{\kappa_1} \end{aligned} \tag{2.1}$$

To perform this parametric study, many solutions of the pertinent differential equation of the domain will be performed. A finited difference method will be used, implemented on a graphics processing unit (GPU) to provide a fast solution, and make a reaonble interpolation of the parameter ranges computable within the time scope of this project.

3. Thermal Diffusion

We start with the thermal diffusivity equation, taken in the steady state case:

$$\rho\, C_p \frac{\partial T(x,y,z,t)}{\partial t} = \nabla \cdot [\kappa(x,y,z) \cdot \nabla T(x,y,z,t)] = 0 \tag{3.1}$$

Due to the spatial variance of κ, we will consider the flux before the divergence operator is applied. This is done becasue $\kappa(x, y, z)$ does not vary smoothly, and had discontinuities between materials; we must consider this as we do the derivative expansions.

$$\nabla \cdot \underbrace{[\kappa(x, y, z) \cdot \nabla T(x, y, z, t)]}_{\text{Flux}} = 0 \tag{3.2}$$

This would be more economically encoded in subscript/superscript Einstien notation, but here equation (3.2) will be explicited expanded in our 3 spatial dimensions :

$$0 = (\frac{\partial}{\partial x}, \frac{\partial}{\partial y}, \frac{\partial}{\partial z}) \cdot [\kappa(x, y, z)(\frac{\partial T}{\partial x}, \frac{\partial T}{\partial y}, \frac{\partial T}{\partial z})] \tag{3.3}$$

$$0 = \frac{\partial}{\partial x} \underbrace{\left[\kappa(x, y, z)\frac{\partial T}{\partial x}\right]}_{F^1(x,y,z)} + \frac{\partial}{\partial y} \underbrace{\left[\kappa(x, y, z)\frac{\partial T}{\partial y}\right]}_{F^2(x,y,z)} + \frac{\partial}{\partial z} \underbrace{\left[\kappa(x, y, z)\frac{\partial T}{\partial z}\right]}_{F^3(x,y,z)} \tag{3.4}$$

Now we can expand these directional flux functions , F^i on a discrete spacing ; we'll use dummy variables $\{x', y', z'\}$ to avoid confusion in the evaluation of the outer divergence operator:

$$F^1(x', y', z') = \kappa(x', y', z') \left[T(x' + \frac{\Delta x}{2}, y', z') - T(x' - \frac{\Delta x}{2}, y', z')\right] \tag{3.5}$$

$$\begin{aligned}\frac{\partial F^1(x', y', z')}{\partial x} &= F^1\big|_{x+\frac{\Delta x}{2}} - F^1\big|_{x-\frac{\Delta x}{2}} \\ &= \kappa(x + \frac{\Delta x}{2}, y, z)\,[T(x + \Delta x, y, z) - T(x, y, z)] - \\ &\quad \kappa(x - \frac{\Delta x}{2}, y, z)\,[T(x, y, z) - T(x - \Delta x, y, z)]\end{aligned} \tag{3.6}$$

Notice that we are now evaluateing κ between grid locations; this can be estimated as:

$$\begin{aligned}\kappa(x + \frac{\Delta x}{2}, y, z) &\approx \frac{1}{2}(\kappa(x + \Delta x, y, z) + \kappa(x, y, z)) \\ \kappa(x + \frac{\Delta x}{2}, y, z) &\approx \frac{1}{2}(\kappa(x - \Delta x, y, z) + \kappa(x, y, z))\end{aligned} \tag{3.7}$$

Now that we have all our values in terms of steps in Δx, we can change everything to an indicial notation, and solve for $T_{i,j,k}$:

$$\begin{aligned}T_{i,j,k} = ((&T_{i,j,k-1} + T_{i,j,k+1} + T_{i,j-1,k} + T_{i,j+1,k} + T_{i-1,j,k} + T_{i+1,j,k})\kappa_{i,j,k} + \\ &T_{i,j,k-1}\kappa_{i,j,k-1} + T_{i,j,k+1}\kappa_{i,j,k+1} + T_{i,j-1,k}\kappa_{i,j-1,k} + \\ &T_{i,j+1,k}\kappa_{i,j+1,k} + T_{i-1,j,k}\kappa_{i-1,j,k} + T_{i+1,j,k}\kappa_{i+1,j,k})/ \\ &(6\kappa_{i,j,k} + \kappa_{i,j,k-1} + \kappa_{i,j,k+1} + \kappa_{i,j-1,k} + \kappa_{i,j+1,k} + \kappa_{i-1,j,k} + \kappa_{i+1,j,k})\end{aligned} \tag{3.8}$$

We can see from the structure of (3.8) that this is indeed a 7-point stencil. By applying this stencil iteratively across our volume, we will ultimately result in a solution that satifies the original PDE.

4. Solver and Implementation

Ranges for the paramters were specified, such that α ranged from [0.1, 10] in 15 equal discrete steps, and η range from [0.3, 3] in 15 discrete equal steps. The domain size is chosen to be $x = [0, 10], y = [0, 10], z = [0, 10]$, providing a cubic RVE. The numerical values use here are not specific, as we have designed a non-dimensional analysis, as mentioned before.

For each value of η, 10 random microstructures were generated. This final loop over several microstructures is critical to account for variable results from the random particle insertion algorithm. Final results are presented averaged across this ensemble of 10 microstructures. Figure 1 shows some examples of the generated microstructures before "gridding" these spheres into a discrete grid for feeding into the solver. Figure 2 show one of these microstructres in it's discretized format.

This ultimately required 2,250 executions of the finite differences solver program. This problem lends itself well to implement on a parallel computation machine, since each grid location value can be updated based on it's surrounding values for each iteration. Solution time for the complete parameter study was approximately 2 hours on an Nvidia GeForce GTX 480 GPU, with each execution having an approximate solution time of 0.5 to 3.5 seconds.

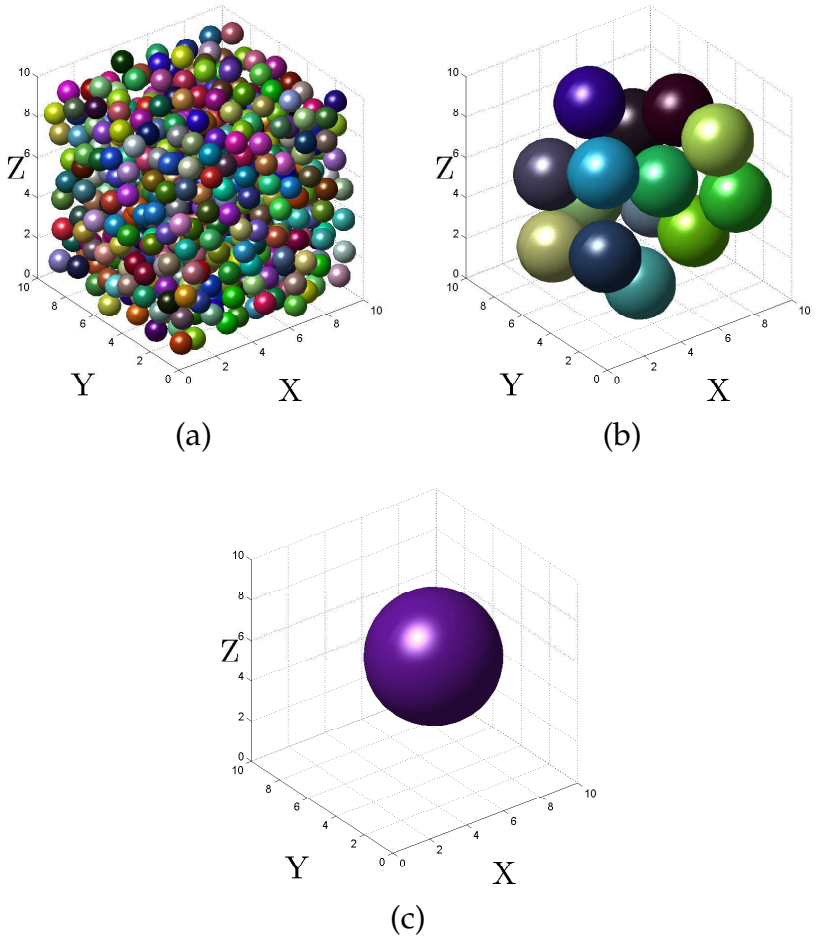

Figure 1: Particle insertsions for (a) η = 0.03 , $N_{\text{part}} = 523$, (b) η = 0.157 , $N_{\text{part}} = 12$, (c) η = 0.3 , $N_{\text{part}} = 1$

To solve this problem, we must impose a boundary condition. It is convenient to specify an isothermal boundary condition, such that:

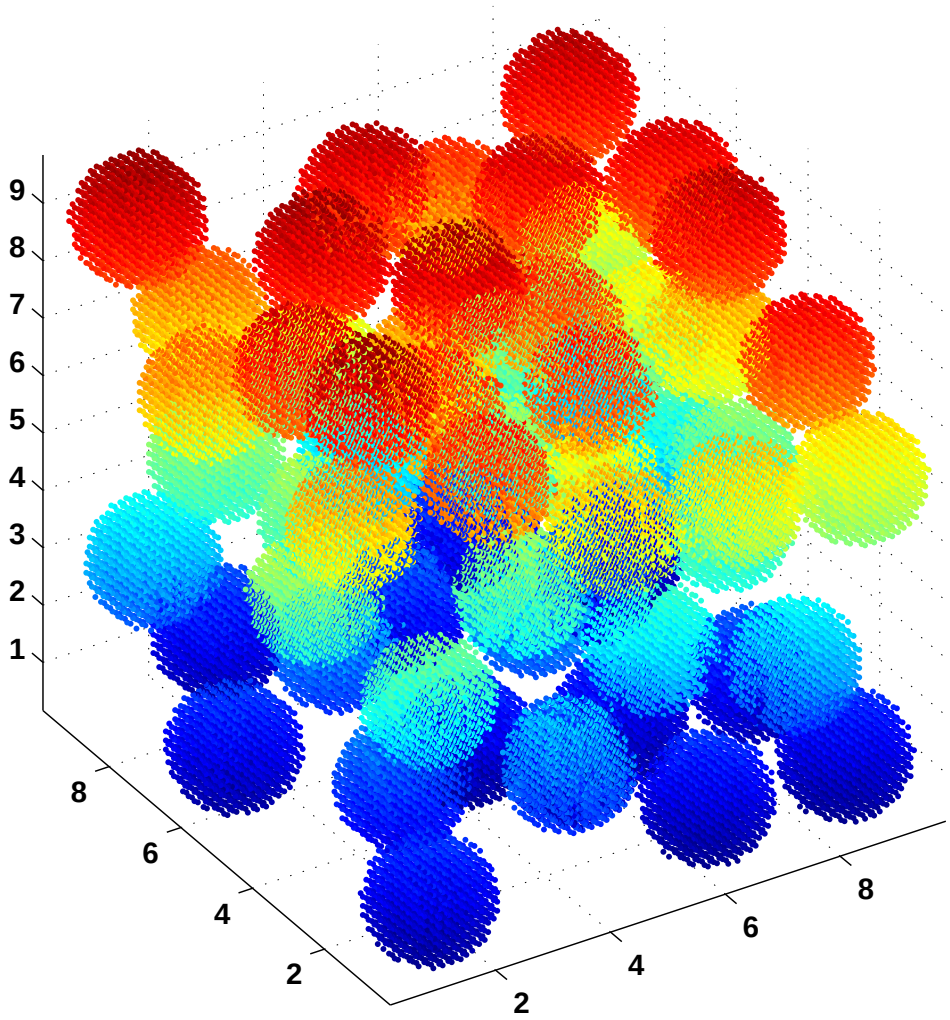

Figure 2: An example of the discretization of a generated microstructure. Only the particle phase is shown here; a 3-dimensions array is generated for $\kappa_{i,j,k}$ from this dataset and the α parameter. Coloring only represent ths z height of the particle in the domain.

$$\begin{aligned} T(x,y,0) &= 0 \\ T(x,y,10) &= 0 \\ T|_{\partial\Omega} &= z/10; \end{aligned} \tag{4.1}$$

This provides an effective isothermal gradient over the thickness of the matieral. Now, our problem is completely specified: running the solver for every parameter pair and microstructure will generate a distribution of $T(x,y,z)$, which can be post-processed to find the effective κ^*. By considering the resulting composite material as effectively isotropic overall, we have that:

$$\kappa^* = \sqrt{\frac{\langle \kappa \nabla T \rangle \cdot \langle \kappa \nabla T \rangle}{\langle \nabla T \rangle \cdot \langle \nabla T \rangle}} \tag{4.2}$$

5. Observations and discussions

The result of the parameter study is shown in Figure 5, giving the ratio between κ^*/κ_1, such that it is non-dimensional and general, as a function of α and η. We can see a "hump" in this surface, which is a continuation of the volume fraction discretization effect, discussed below. In light of this, it is more appropriate to consider the results in terms of the particle volume fraction v_2 and α, which is shown in Figure 6; this represents equivalent information, since v_2 is wholly dependant on η.

As mentioned earlier, the algorithm for microstructure generation by randomly inserting spheres into a domain may be insufficient to properly model a much larger sample volume with this RVE. At large values of η, where R is the particle radius, and $V(1/3)$ is the edge length of our domain since we are using a cubic RVE volume, very few particles are inserted into our model domain. Because particles must be wholly inside the domain boundary, we see a volume fraction quantization for these large particles, with some generated microstructures only have a single large particle in them.

The Hashin-Shtrikman bounds for thermal diffusivity are given in (5.1), along with a mixing based on a θ parameter. By substituting for our parameters defined in (2.1) and solving for θ, we can convert our results shown in Figure 5 into a surface plot for the value of θ, shown in Figure 7. This serves to compare the calculated properties to these established bounds. The shape of this surface indicated that a choice of a constant value of θ for mixing these bounds to estimate the effective properties may be a poor choice.

$$\begin{aligned} \kappa^{*,-} &= \kappa_1 + \frac{v_2}{\frac{1}{\kappa_2-\kappa_1} + \frac{v_1}{3\kappa_1}} \\ \kappa^{*,+} &= \kappa_2 + \frac{v_1}{\frac{1}{\kappa_1-\kappa_2} + \frac{v_2}{3\kappa_2}} \\ \kappa^{*,-} &\leq \kappa^* \leq \kappa^{*,+} \\ \kappa^* &= \theta\kappa^{*,+} + (1-\theta)\kappa^{*,-} \end{aligned} \tag{5.1}$$

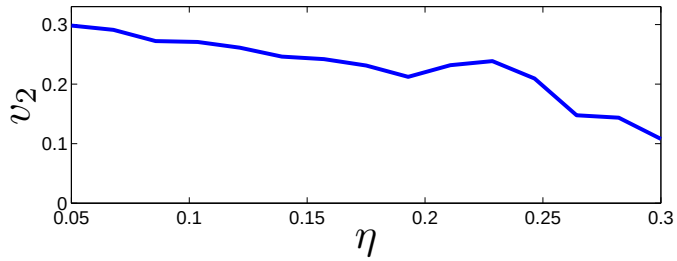

(a)

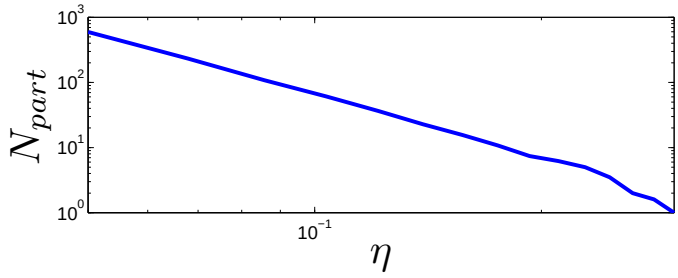

(b)

Figure 3: Results of microstructure generation, showing (a) particle volume fraction and (b) number of particles present in the RVE.

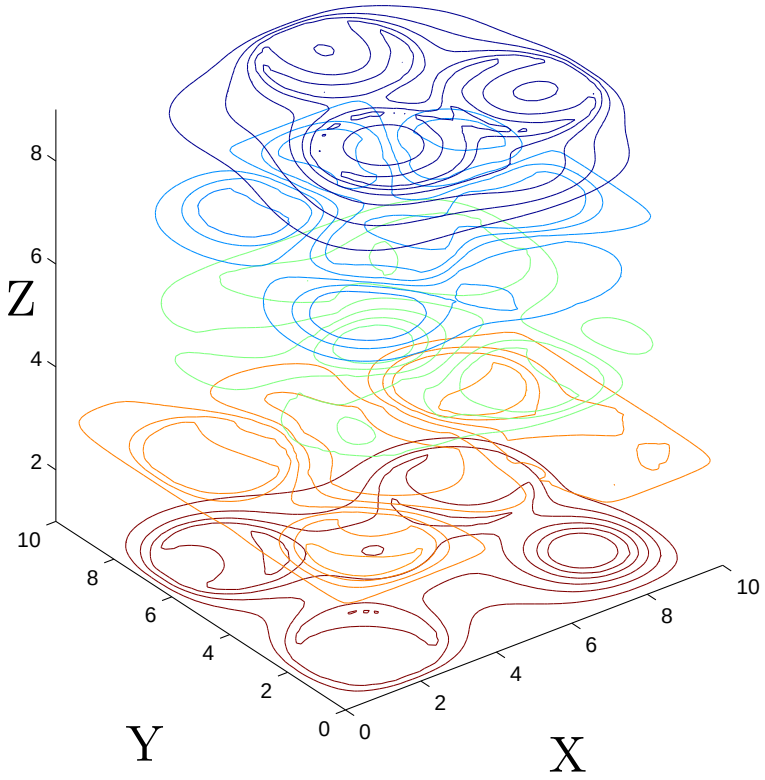

Figure 4: Isocontours at several z levels of a single reslting temperature distribution for η = 1.75, $\alpha = 3.64$, where there are 12 particles in the RVE.

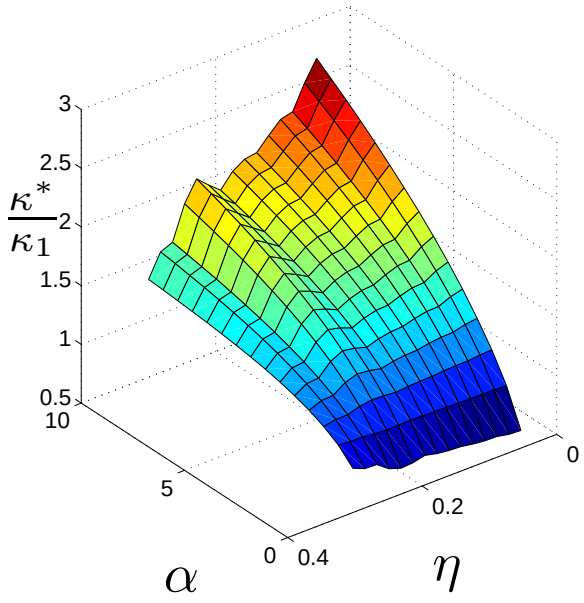

Figure 5: The resulting output of the parametric study, as a function of particle-to-domain size ratio, η, and the property mismatch parameter α.

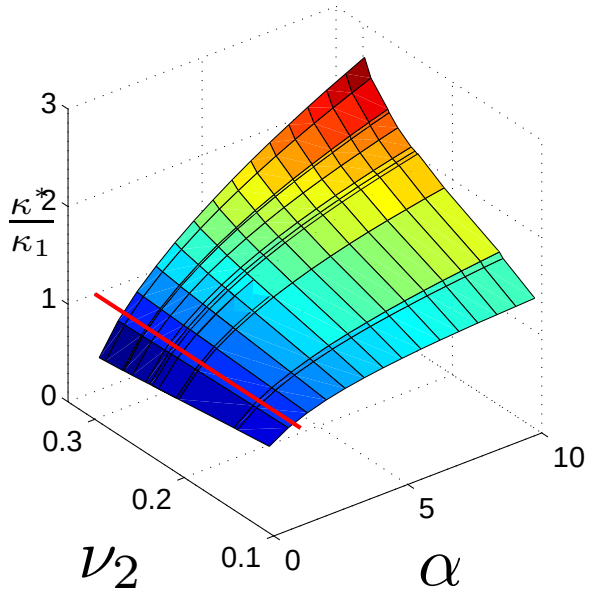

Figure 6: The resulting output of the parametric study, as a function of particle volume fraction and the property mismatch parameter α. The red line corresponds to α = 1, where we expect and find that $\kappa^*/\kappa_1 = 1$

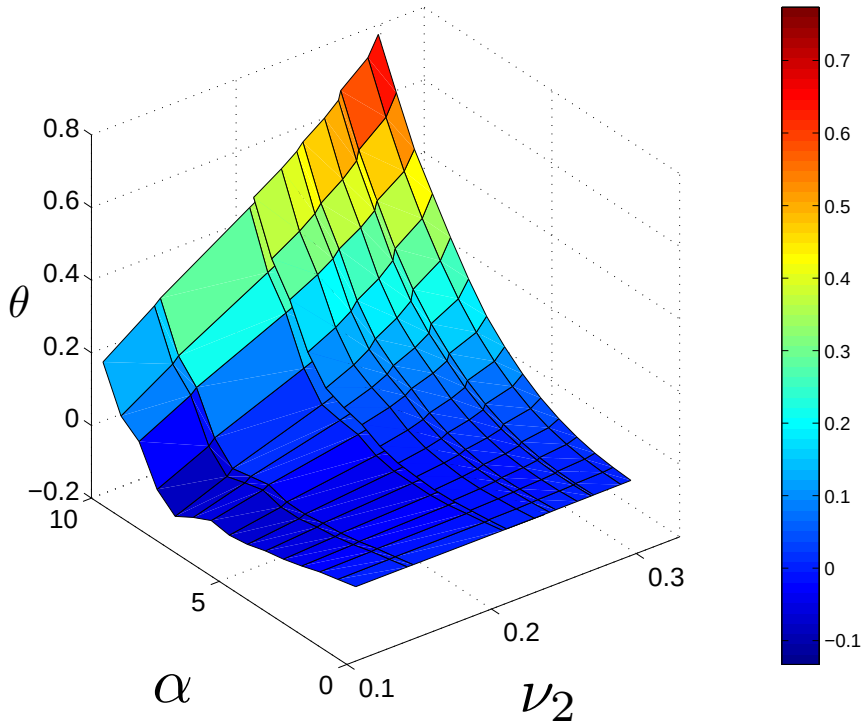

Figure 7: Calculated effective θ from Equation (5.1).

6. Conclusions

The resulting tabulation of κ^* would be sufficient to provide an interpolation of the investigated domain. This could now be a reference for the design of materials with a specifically required thermal performance.

We have arrived at several convincing validations of the formulation used herein: when considering the results in terms of η, we see a quantization effect that is elided by reconsidering the solutions as a function of v_2, where we effectively see the resulting surface "overlap" itself, indicating consistency. It is also seen that for α, the value of $\kappa^*/\kappa_1 \approx 1$, for which our RVE is reduced to a homogenous isotropic material.

It has been observed the closed form Hashin-Shtrikman bounds for this material are of limited use when considering a large range of paramters, as the θ mixing parameter can vary from approximately $[0, 0.8]$. This also shows us that choosing a constant value of θ to provide an estimate of κ^* may give a poor estimation.